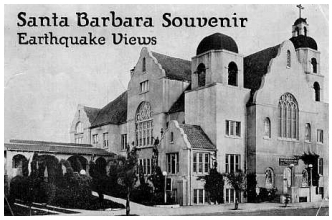

4th IASPEI / IAEE International Symposium:

Effects of Surface Geology on Seismic Motion

August 23–26, 2011 · University of California Santa Barbara

ESTIMATION OF VELOCITY DISCONTINUITIES IN SEDIMENT OF YOKOHAMA REGION BY APPLYING NONSTATIONARY RAY DECOMPOSITION METHOD TO YOKOHAMA ARRAY RECORDINGS

Makiko TAKAGISHI
Yokohama City University
22-2 Seto, Kanazawa-ku, Yokohama
Kanagawa, 236-0027 Japan

Shigeo KINOSHITA
Yokohama City University
22-2 Seto, Kanazawa-ku, Yokohama
Kanagawa, 236-0027 Japan

ABSTRACT

We estimated the velocity boundaries in a sedimentary layer in Yokohama by applying the nonstationary ray decomposition (NRD) method to strong motion data recorded by the Yokohama dense strong motion (YKH) array, expanding the investing field south-southeast of the FCH array. In the NRD method, we estimate the velocity boundaries of the real layered structure from surface recordings by decomposing the power of an SH-wave into the instantaneous power of the wave associated with rays in a homogeneous half space. The estimated results are represented as a function of lapse time and depth time, which is the travel time from the surface toward the depth direction. The proposed statistical nonstationary ray decomposition (SNRD) method is herein used to estimate the velocity boundaries statistically.

INTRODUCTION

One of the most important problems in strong motion prediction is to evaluate the ground structure quantitatively because the prediction is conducted based on waves synthesized from the velocity profiling. In metropolitan areas such as Los Angeles, Osaka, and Tokyo, the ground structure from the surface to the pre-Tertiary basement affects strong motions. Therefore, we need to determine the ground structure.

A 2D-velocity structure model was constructed in the 1970s. Velocity boundaries were estimated in sediment for long-period motions of more than 2 s (Horike, 1998). In metropolitan areas such as Tokyo and Yokohama, refraction explorations using artificial seismic sources and microtremor explorations using array observations were conducted, revealing an outline of the velocity structure. Toriumi (1980) analyzed seismic array data in the Osaka basin and indicated that the long duration of seismic motion is caused by surface waves generated at the basin edge. Thus, irregular subsurface structure should be evaluated quantitatively. Horike *et al.* (1990) reported that this irregular structure cannot be expressed precisely using the 2D-subsurface structure model, although the results obtained by synthesized and observed waves did not match well.

In the 1980s, several researchers constructed 3D-subsurface structures. Although several explorations were conducted using various methods, the precision of the estimated results was not sufficient to construct the 3D-velocity structure, and explorations were conducted in only a few areas, such as Tokyo, Osaka, and Nagoya. Therefore, dense and precise explorations are required.

Starting from the 1990s, velocity profiling using natural seismic sources has been conducted beneath the site, e.g., velocity profiling using receiver functions (e.g., Langston, 1979, Miura and Midorikawa, 2001) and seismic interferometry (e.g., Claerbout, 1968, Nakahara, 2006, Yoshimoto *et al.*, 2010). An advantage of using natural earthquakes as seismic sources is the ability to use SH-waves. S-wave measurement is easier than P-wave measurement, and SH-waves do not generate converted waves such as P- and SV-waves. These estimation methods are suitable for estimating deep velocity boundaries, such as the upper boundaries of the mantle and the pre-Tertiary basement.

Recently, as a new method for estimating velocity boundaries using natural seismic sources, the nonstationary ray decomposition method (NRD method) was proposed by Kinoshita (2009). In the NRD method, we decompose the power of an SH-wave into the instantaneous power associated with rays in a homogeneous half space. The estimated results obtained by applying this method to seismograms are represented as a function of the lapse time and the depth time, which is the travel time from the surface in depth direction. This method was evaluated by Takagishi and Kinoshita (2011b), who applied it to the FCH array seismograms, and the

estimated results of velocity boundaries were in agreement with the results of S-wave profiling obtained by Yamamizu *et al.* (1981) using the down-hole method. In this method, we can estimate several boundaries, such as the upper boundaries of the pre-Tertiary basement and the Kazusa and Miura group. Zheng *et al.* (2011) also applied this method to ground motion data recorded at 12 stations in the Kanto region and estimated the depth of the upper boundaries of the pre-Tertiary basement. The estimated results were in agreement with the results obtained by the VSP method (Yamamizu, 2004).

In the present study, we estimated the velocity boundaries in a sedimentary layer in the Yokohama region by applying the NRD method to the strong motion data recorded at the Yokohama dense strong motion network (YKH array), expanding the investing field south-southeast of the FCH array. In the case of strong motion data recorded at the FCH array, the determination of velocity boundaries was not difficult because the reflected phases were easily identified. On the other hand, reflected phases recorded in the Yokohama region are masked by multi-reflected waves generated in the soft subsurface. Thus, the identification of these reflected waves will be difficult. Furthermore, the depth of the top boundary of the pre-Tertiary basement has not yet been measured. For these reasons, we attempted to estimate the velocity boundaries in this area. We also estimated the velocity boundaries using the NRD method in a statistical manner, by means of the statistical nonstationary ray decomposition (SNRD) method proposed herein.

DATA

We expanded the investing field beyond the Fuchu area to the Yokohama region located south-southeast of the FCH array, as shown in Fig. 1. The new field is a rectangular area with a width of 4 km and a length of 40 km, which encloses 37 stations of the Yokohama dense strong motion network (YKH array), the KNGH10 site (in KiK-net), which has a 2,000-m borehole, and the SYR site (in SK-net), as shown in Fig. 1. Open circles and crosses indicate stations of the FCH (except for the FCH site) and the YKH array (except for the kz12u site), respectively. The blue triangle and black diamond symbols indicate the SYR and the KNGH10 sites, respectively. The two red diamonds indicate the FCH site and the YCU (kz12u) site. The width of the new investing field corresponds to the radius of the FCH array.

The YKH array consists of 150 sites with a station-to-station distance of approximately 2 km. This is the densest array in Japan and was constructed in 1996 for earthquake disaster mitigation after the Kobe earthquake in 1995 (Takahide *et al.,* 2002, Midorikawa, 2005). High-precision digital acceleration seismographs are used to acquire ground motions ranging from weak to strong. Ground acceleration of up to 2g is measured with 24-bit A/D resolution at a sampling rate of 200 Hz. Although the results of the velocity structure at the KNGH10 site investigated using the down-hole method did not reveal the upper boundary of the pre-Tertiary basement, an apparent velocity boundary in sediment was recognized (Suzuki and Komura, 1999). Thus, the upper boundary of the pre-Tertiary basement is expected to be deeper than 2 km.

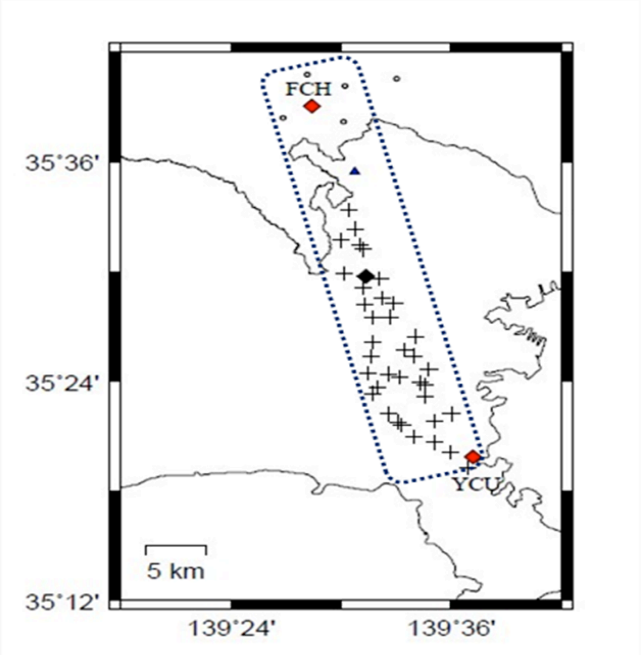

Fig. 1.The map of the Yokohama region

A total of 1,361 recordings were obtained for the 49 earthquakes that occurred in the Kanto area from 2000 to 2005. The data were obtained for the events having JMA magnitudes in the range of from 3.7 to 6.0. In Fig. 2, the star symbol, the dotted line, and the cross symbols indicate the KNGH10 site, the survey line shown in Fig. 1, and the epicenters of these earthquakes, respectively.

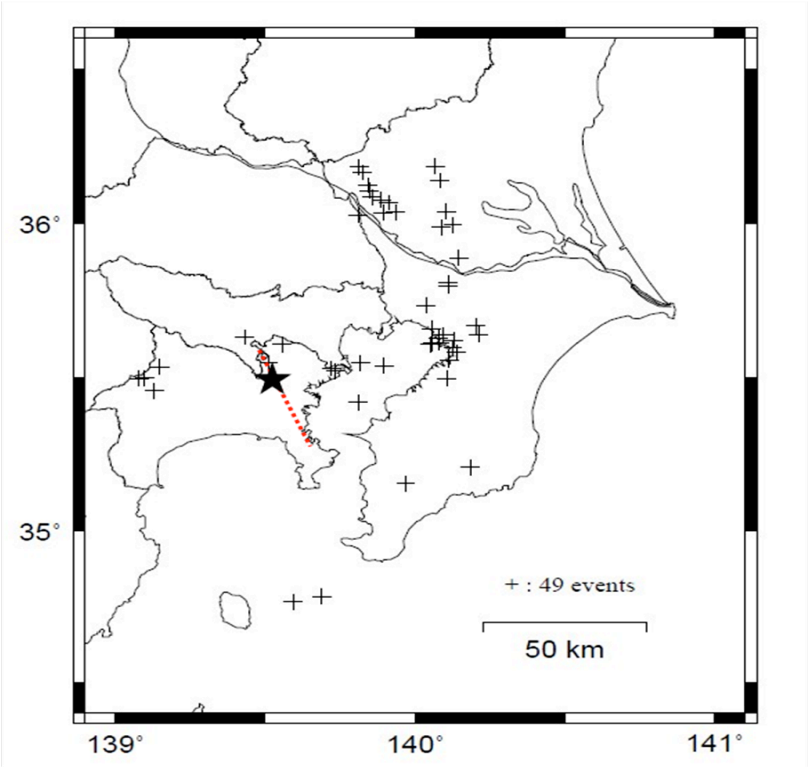

Fig. 2. Epicenters of 49 earthquakes used in the present study.
The star symbol and the dotted line indicate the KNGH10 site and the survey line shown in Fig. 1., respectively.

METHOD

In the present study, we estimated the velocity discontinuities in sediment by applying a nonstationary ray decomposition method (NRD method) to surface recordings as discussed in the previous section. The method yields the estimates of velocity boundaries for real layered structures from surface seismograms by decomposing the power of an SH-wave into the instantaneous power of waves associated with rays in a homogeneous half space. The estimated results are presented as a function of lapse time t and depth time τ, which is the travel time from the surface toward the depth direction. The reflected phases of the SH-wave are visualized in this (t,τ) map, in which the velocity boundaries are shown by local maxima.

A flowchart for estimating velocity boundaries is shown in Fig. 3, and the procedures are described hereinafter. First, we converted the three components (NS, EW, and UD) of acceleration data recorded at the surface to velocity data using an integration filter (a bandpass filter). Using horizontal components of velocity data, we approximated the particle motion as an ellipse, assuming the major axis to be along the transverse direction. Hereinafter, we consider the transverse components of data (SH-wave). This procedure follows the method proposed by Fukushima *et al.* (1992). We then performed preprocessing for the transverse component of the data in order to identify the reflected phases in the estimated (t,τ) map. The preprocessing will be explained in the following section.

A data window of 20.48 s in length was selected as follows. The data $x(t)$ is composed of the data starting from 5 s before the onset of the direct S-wave to 15.8 s of after the onset of the direct S-wave, as determined visually. Then, $x(t)$ was converted into an analytic signal, $x_a(t)$. The signal is defined as follows:

$$x_a(t) \equiv x(t) + iH[x(t)] \tag{1}$$

where $H[x(t)]$ is the Hilbert transform of $x(t)$. The analytic signal $x_a(t)$ is used to prevent the aliasing effects of the negative Fourier components of the real-valued signal and to suppress the cross term of the Wigner-Ville distribution (Cohen, 1995) at low frequencies (Claasen and Mecklenbrauker, 1980). We calculated the Wigner-Ville distribution using the analytic signal $x_a(t)$. The Wigner-Ville distribution is defined as follows:

$$W(t,f) = \int_{-\infty}^{\infty} R(t,\tau) e^{-i2\pi f t} dt \tag{2}$$

In this relation, $R(t,\tau)$ is given by

$$R(t,\tau) = x_a(t+\tau/2)x_a(t-\tau/2) \tag{3}$$

The instantaneous power associated with the rays at lapse time t and depth time τ in a homogeneous half space is calculated using the above Wigner-Ville distribution and is given as follows:

$$\left|x^{(\pm)}(t,\tau)\right|^2 = \int [W(t+\tau,f) + W(t-\tau,f) \pm 2W(t,f)\cos(2\tau f)]df \tag{4}$$

The instantaneous power is calculated by frequency integration of three Wigner-Ville distributions at three lapse times: $t+\tau$, $t-\tau$, and t . The first, second, and third terms on the right-hand side of the equation are the Wigner-Ville distributions for up-coming waves and down-going waves and the interaction of both waves, respectively. The + and – symbols in the term $x^{(\pm)}(t,\tau)$ on the left-hand side of the relation indicate the sum and the difference, respectively, of up-coming and down-going waves and correspond to the sign of the third term in the right-hand side of relation (4). We hereinafter consider only the velocity normalized strain wave, i.e., the $x^{(-)}(t,\tau)$ wave (Kinoshita, 2009). When the S-wave velocity at the lower layer is higher than that at the upper layer at the velocity boundary, the instantaneous power generates local maxima. The estimated instantaneous power is displayed on the (t,τ) map, in which the horizontal and vertical axes indicate the lapse time t and depth time τ, respectively. In interpreting the (t,τ) map, we determined the travel time from surface to velocity boundaries by reading the depth times τ at the local maxima. We also validated the reflected phases using surface seismograms and the Wigner-Ville distribution.

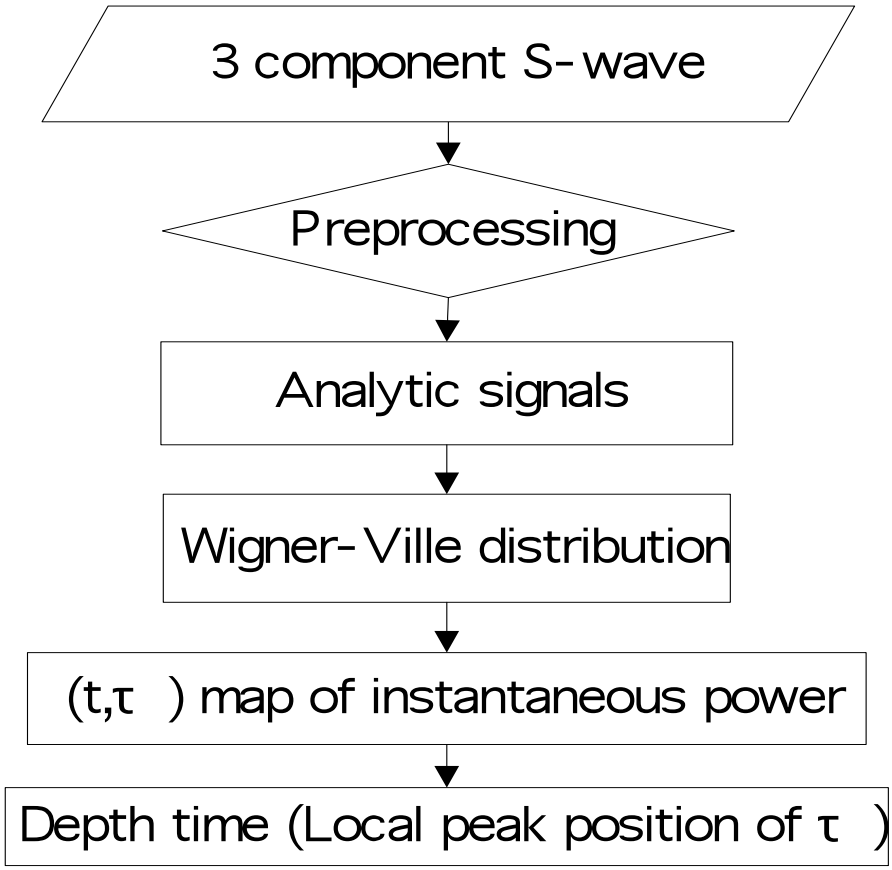

Fig. 3. A flowchart for estimating the (t, τ)map

Bandpass filtering by using intrinsic mode functions (IMFs)

As a preprocessing process by which to facilitate the detection of the reflected phases on the (t,τ) map, we applied bandpass filtering using intrinsic mode functions (IMFs) constructed from the transverse component of data. This procedure follows Huang and Shen (2005).

The empirical mode decomposition method (EMD method) is used to analyze nonstationary time series. In the EMD method, we decomposed the data into a set of simple oscillatory functions with different center frequencies, defined as intrinsic mode functions (IMFs). An IMF must satisfy the conditions whereby the number of extrema must be equal to the number of zero crossings (or differ by at most one), and the mean value of the envelope functions is zero. The IMF can be obtained by repeated application of an iterative procedure called shifting. For example, the first IMF $c_1(t) = shifting[x(t)]$ can be obtained by shifting $x(t)$, where $x(t)$ is the measured time series data. The second IMF is then equal to $c_2(t) = shifting[x(t) - c_1(t)]$, and so on. As a result, we have

$$x(t) = \sum_{k=0}^{n} c_k(t), \tag{5}$$

which indicates that the measured time series data can be decomposed into *n* empirical modes, each of which satisfies the conditions of an IMF, plus a residual term $c_0(t)$. In general, since *n* is a small number, the method efficiently decomposes the data into IMFs. As a result, IMFs are a bank of bandpass-filtered waves. Thus, the summation of successive IMFs produces a bandpass-filtered wave with a bandwidth determined by the provided IMFs.

Example

As an example for estimating velocity boundaries using a (t,τ) map, we present the results obtained at the kz02s site (139.62E, 35.42N) using the records for an earthquake that occurred in northwestern Chiba prefecture (140.134E, 35.576N) with a JMA magnitude of 6.0 and a focal depth of 73 km.

Figure 4(a) shows the original SH-wave with a duration of 20.48 s. Using the EMD method, we decomposed the wave into 11 IMFs, and summed three IMFs, namely, C3, C4, and C5, as shown in Figs. 4(b), 4(c), and 4(d), respectively. The frequency band was from 2.24 to 3.5 Hz. This bandpass-filtered wave, which was used to estimate the instantaneous power, is shown by the thick black line in Fig. 4(e) and the dotted line in the figure indicates the original SH-wave. The bandpass-filtered signal was converted to the analytic signal $x_a(t)$ by the Hilbert transform, and the Wigner-Ville distribution was then calculated by relation (2). The instantaneous power associated with rays in a homogeneous half space was calculated by relation (4), and the resulting (t,τ) map is shown in Fig. 5(b). The direct S-wave is labeled as S0 in this figure. The local maximum appears at a lapse time of 11 s and a depth time of 2.7 s. This is the reflecting point at the pre-Tertiary basement (M-B), which is hereinafter referred to as phase S2. We can identify this phase in the SH-wave in Fig. 5(a). Another reflection, which is thought to correspond to the K-M boundary, occurs at a lapse time of 9 s and a depth time of 1.7 s.

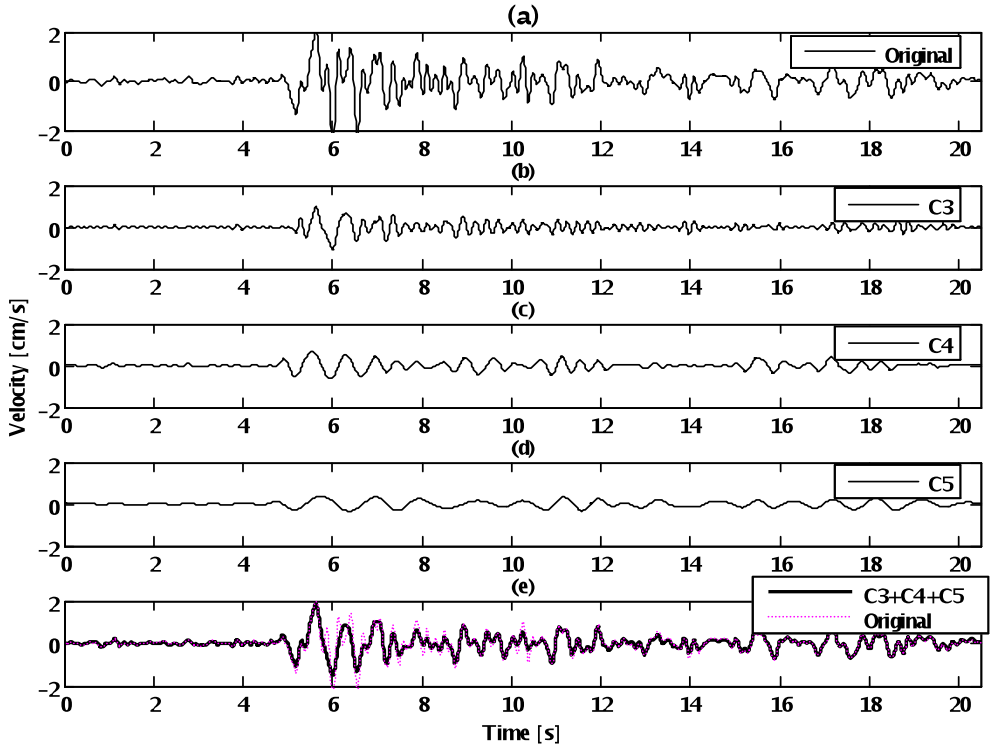

Fig. 4. SH-velocity waves recorded at the kz02s site: (a) original SH-wave, Figs. 4(b),4 (c), and 4(d) are IMFs with different center frequencies decomposed from the wave shown in Fig. 4(a). Fig. 4(e) is the bandfiltered wave composed of summation of three IMFs.

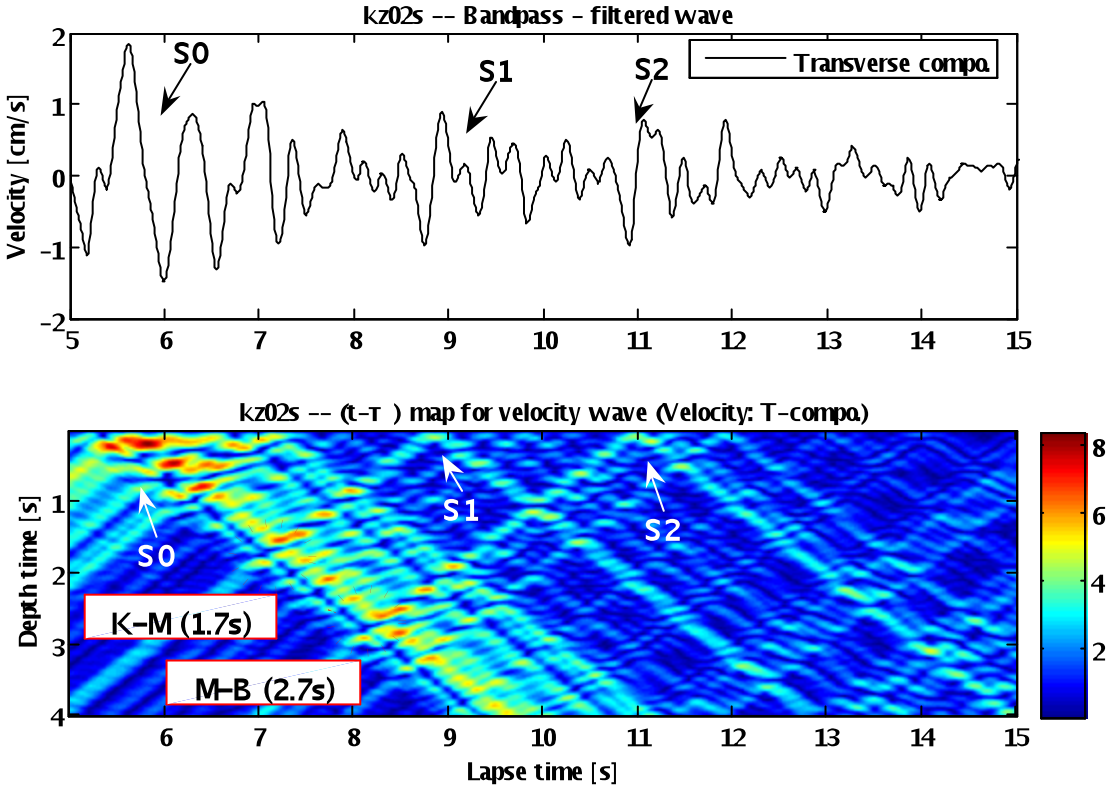

Fig. 5. An example of SH-velocity wave(Fig. 5(a)) and the estimated (t, τ) map of normalized instantaneous power associated with rays in a homogeneous half space (Fig. 5(b)). Labels S0, S1, and S2 correspond, respectively.

RESULTS

Figure 6 shows the estimated depth time τ from the surface to the major boundaries in the basement-sedimentary layer system. The horizontal axis shows the latitude, and the vertical axis shows the depth time τ from the surface. The results are for the Kazusa and Miura groups (K-M, asterisk) and the Miura group and the pre-Tertiary basement boundaries (M-B, open circle), respectively. Smoothed boundaries using fifth-order polynomials are indicated by dotted lines. The estimated depth time of K-M and M-B obtained at the FCH array (Takagishi and Kinoshita, 2011b) are also plotted in the left-hand side of Fig. 6.

The following are novel findings of the present study. First, we were able to estimate two velocity boundaries, one of these boundaries is in sediment (K-M) and the other is the upper boundary of the pre-Tertiary basement (M-B). However, we could not estimate the subsurface-Kazusa group boundary (S-K), which is the closest boundary to the surface. The reason for this was the difficulty in identifying reflected phases by eye due to the masking effect of reflected waves in the soft subsurface. In order to estimate the S-K boundary, the modification of the NRD method will be discussed later. Second, the depth time τ at the K-M and M-B boundaries gradually increased along the line from the FCH array to the KNGH10 site in Fig. 6 and increased the most at latitude of 35.4 degrees in the southern Yokohama region. Then, both depth times became slightly shallower at the southern part of Yokohama, as indicated by the two dotted lines in Fig. 6. Thus, on the whole, the upper boundary of the pre-Tertiary basement (M-B) is dipping towards a deeper direction (toward the south-southeast direction) from FCH to YKH. The depth times at K-M and M-B were from 1.5 to 2.2 s and from 2.4 to 3.2 s, respectively. The depth times for the two velocity discontinuity boundaries were found to change synchronously from the FCH array to Yokohama. The results obtained using the NRD method for the M-B boundary were consistent with those obtained using receiver functions, as reported by Miura and Midorikawa (2001).

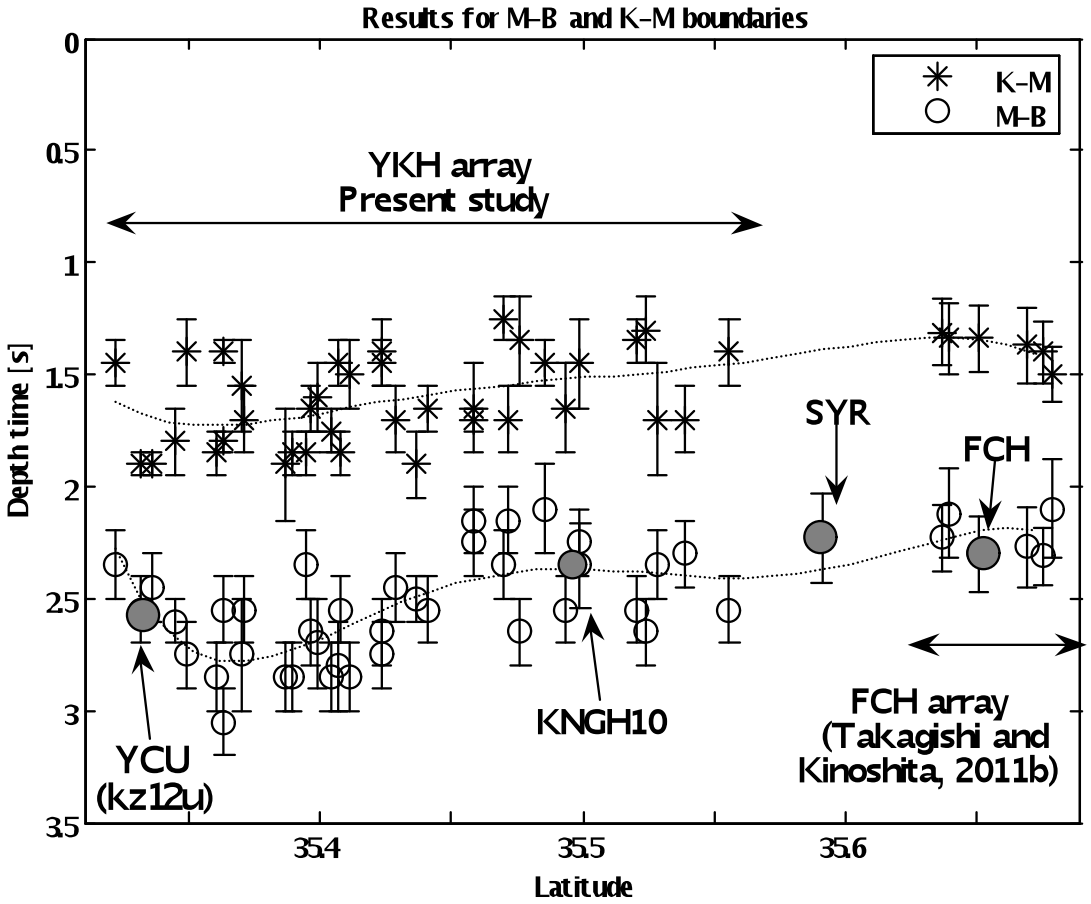

Fig. 6. The estimated results of FCH-YCU line. Horzontal and vertical axises are latitude and depth time [s], respectively. The Results are the upper boundaries of Miura (K-M, astarisks) and the pre-Tertiary basement(M-B, open circles).

EXTENSION OF NRD METHOD

As an extension of NRD method, the estimation of velocity discontinuities was conducted by using NRD method in a statistical sense; that is statistical nonstationary ray decomposition method (SNRD method) (Takagishi and Kinoshita, 2011a).
We applied SNRD method to the data recorded at 80 stations of the YKH array for the 2011 off the Pacific coast of Tohoku earthquake (143.15E, 38.03N: Mw = 9.0, Focal depth: 24 km). Although at first, we applied the ordinary NRD method to the data recorded in this event was applied to the data to estimate the velocity boundaries in sediment, it was difficult to identify the reflected phases of the (t,τ) map. Thus, the statistical analysis of the NRD method was required as follows.

First, the data were divided into a set of subdata with a window length of 20 s. Then, estimation of instantaneous power was conducted following the steps of the section in METHOD, and estimated instantaneous power is represented as $P(t,\tau)$. We estimated local instantaneous power $P_L(\tau)$ as a function of depth time τ by integrating the instantaneous power $P(t,\tau)$ along lapse time t given by relation (6). Then, we normalized the local instantaneous power $P_L(\tau)$ using the total power P_T (relation (7)) which was estimated in the whole (t,τ) plane as shown in relation (8). As an extension of the NRD method, velocity discontinuities were estimated using the NRD method in a statistical manner, i.e., the statistical nonstationary ray decomposition method (SNRD method) (Takagishi and Kinoshita, 2011a).
We applied the SNRD method to the data recorded at 80 stations of the YKH array for the 2011 off the Pacific coast of Tohoku earthquake. We first applied the ordinary NRD method to the data recorded during this event to the data in order to estimate the velocity boundaries in sediment. Identifying the reflected phases of the (t,τ) map was difficult. Thus, statistical analysis of the NRD method was required.
First, the data were divided into a set of subdata with a window length of 20 s. The instantaneous power was then estimated (denoted hereinafter as $P(t,\tau)$) according to the procedure described in the METHOD section. We estimated the local instantaneous power $P_L(\tau)$ as a function of depth time τ by integrating the instantaneous power $P(t,\tau)$ over the lapse time t given by relation (6). We then normalized the local instantaneous power $P_L(\tau)$ using the total power P_T (relation (7)), which was estimated in the entire (t,τ) plane, as shown in relation (8).

$$P_L(\tau) = \int P(t,\tau)dt \tag{6}$$

$$P_T = \iint P(t,\tau)dtd\tau \tag{7}$$

$$P_L(\tau)/P_T = \int P(t,\tau)dt / \iint P(t,\tau)dtd\tau \tag{8}$$

We applied these procedures to each subdata window and then estimated the average normalized local instantaneous power $F(\tau)$ as a function of depth time τ as follows:

$$F(\tau) = \left\langle P_L(\tau)/P_T \right\rangle \tag{9}$$

Thus, we were able to obtain the velocity boundaries from the local maxima of $F(\tau)$. Although we had to analyze numerous strong motion data in order to estimate the velocity boundaries in the ordinary NRD method, we can estimate the velocity boundaries using data for only one event in the SNRD method. This will make the NRD method more convenient.

Figure 7 shows an SH-velocity wave recorded at the kz07s site (139.619E, 35.353N). The rectangular area in Fig. 7 was divided into 11 subdata sets with a window length of 20 s, and the onset time for the rectangular area was determined by the displacement data obtained by integrating the velocity data. Figure 8 indicates the average normalized local instantaneous power obtained by the SNRD method. This figure represents $F(\tau)$ as a function of depth time τ. Three local maxima are easily determined in this figure. These three maxima are the S-K, K-M, and M-B boundaries. Figures 9(a), 9(b), and 9(c) show the results for the M-B, K-M, and S-K boundaries, respectively. The depth times at the boundaries are 2.3 to 3.2 s, 1.0 to 2.0 s, and 0.2 to 0.6 s, respectively.

We were able to estimate the velocity boundaries in sediment using the SNRD method. In particular, the S-K boundary was better estimated using the SNRD method, as compared to the ordinary NRD method. The SNRD method will be a useful as a tool for compensating for the ordinary NRD method.

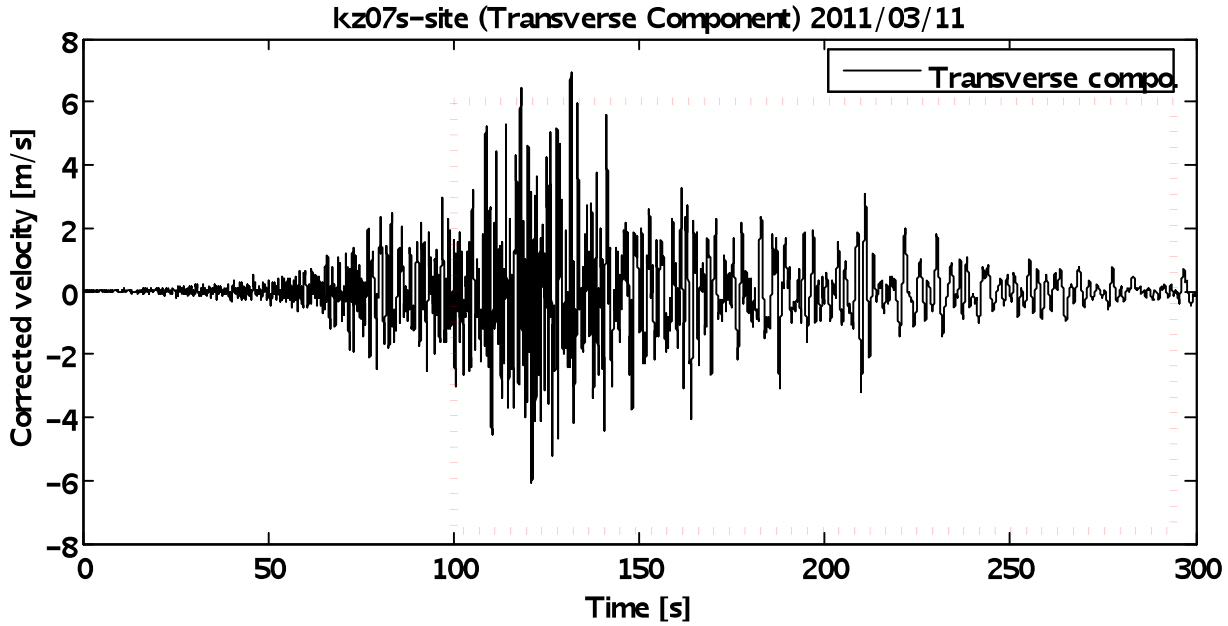

Fig. 7. An example of SH-velocity wave recorded at kz07s site. We divided the data (red rectangular area) into 11 subdata sets with a window length of 20 s and estimated the instantaneous power for each dataset.

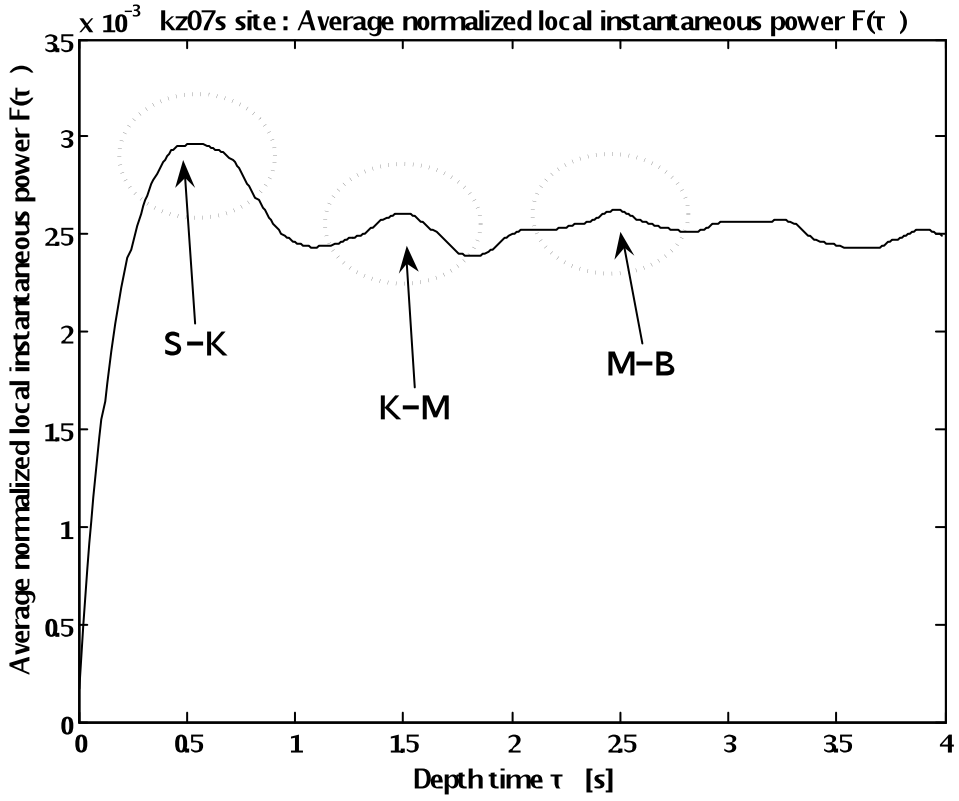

Fig. 8. The average normalized local instantaneous power of the kz07s site. Local maxima correspond to velocity boundaries of S-K, K-M and M-B, respectively.

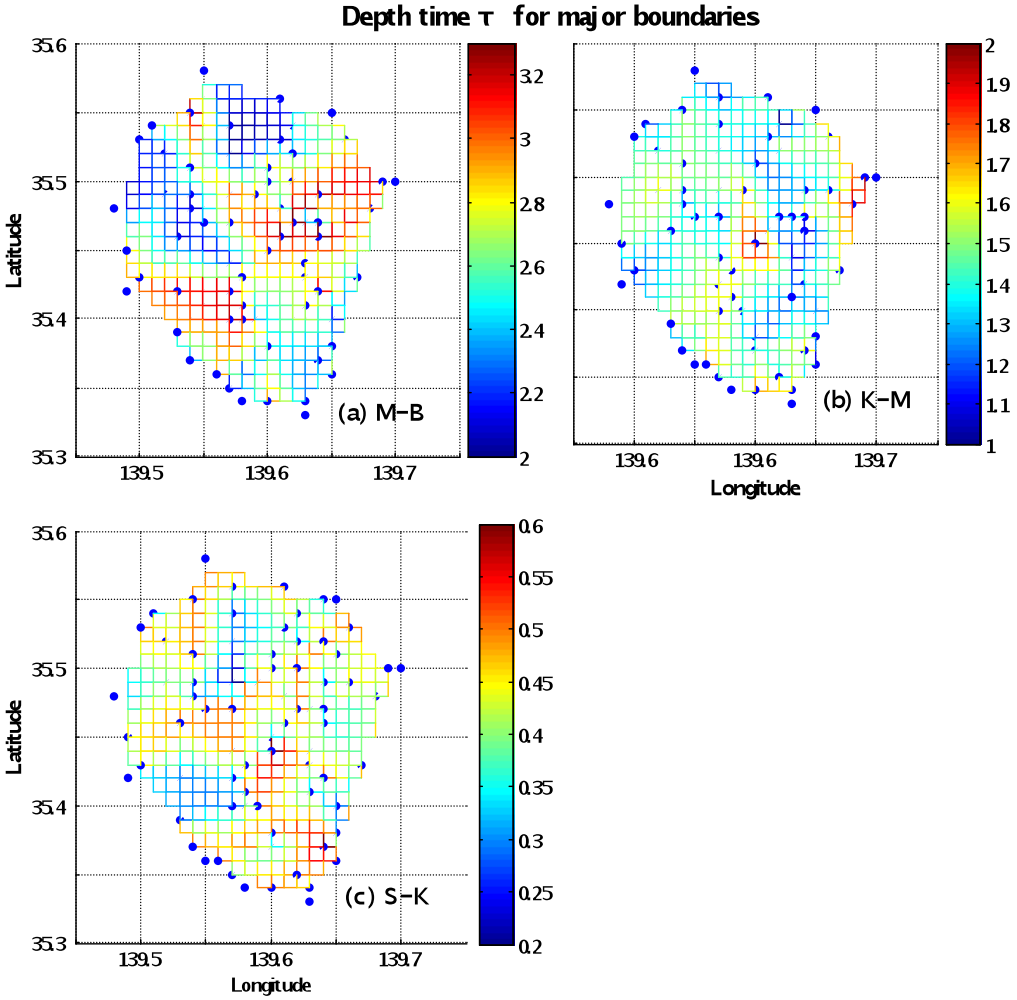

Fig. 9. Estimated results of depth time for major boundaries in the Yokohama region. Figures 9(a), 9(b), and 9(c) indicate the upper boundaries of the pre-Tertiary basement (M-B), the Miura (K-M), and the Kazusa (S-K) group boundaries, respectively. The results are shown using contour map, and a unit of color bars at each map is in seconds.

CONCLUSIONS

We estimated the velocity boundaries in a sedimentary layer in Yokohama by applying the nonstationary ray decomposition (NRD) method to the strong motion data recorded at the Yokohama dense strong motion network (YKH array). The conclusions of the present study are as follows:

1) As preprocessing to facilitate the identification of the reflected phases on the (t,τ) map, we applied bandpass filtering using intrinsic mode functions (IMFs) constructed from seismograms.

2) We were able to estimate two velocity boundaries, one in sediment (K-M) and the other being the upper boundary of the pre-Tertiary basement (M-B). On the whole, the upper boundary of the pre-Tertiary basement is dipping toward the south-southeast. The estimated depth times at K-M and M-B were from 1.5 to 2.2s and from 2.4 to 3.2 s, respectively. The depth times for two velocity discontinuity boundaries were revealed to change synchronously from the FCH array area to Yokohama. However, we were not able to estimate the subsurface-Kazusa group boundary (S-K), which is a near-surface boundary, because the reflected phases are masked by multi-reflected waves generated in the soft subsurface.

3) We also estimated the velocity discontinuities using the newly proposed statistical nonstationary ray decomposition (SNRD) method. The SNRD method was able to better estimate the S-K boundary, as compared to the ordinary NRD method. The SNRD method is thus expected to be a useful tool for compensating for the ordinary NRD method.

ACKNOWLEDGEMENT

We used seismograms of the Yokohama dense strong motion network obtained by Yokohama City. Seismograms recorded at the SYR site of S-K net of the Earthquake Research Institute of the University of Tokyo and the KNGH10 site of KiK-net of the National Research Institute for Earthquake Science and Disaster Prevention were also used in the present study.

REFERENCES

Claasen T. A. C. M. and W. F. G. Mecklenbrauker [1980], ‘‘The Wigner distribution – A tool for time-frequency analysis. Part I: Continuous-time signals’’, Philips J. Res., Vol.35, pp.217-250.

Claerbout, J. [1968], ‘‘Synthesis of a layered medium from its acoustic transmission response’’, Geophysics, Vol.33, pp.264-269.

Cohen, L. [1995], *‘‘Time- frequency analysis’’*, Prentice-Hall, Inc., New Jersey, the U.S.

Fukushima, Y., S. Kinoshita, and H. Sato [1992], ‘‘Measurement of Q^{-1} for S waves in mudstone at Chikura, Japan: comparison of incident and reflected phases in borehole seismograms’’, Bull. Seism. Soc. Am. Vol.82, pp.148-163.

Horike, M. [1985], ‘‘Inversion of phase velocity of long-period microtremors to the S-wave-velocity structure down to the basement in urbanized areas’’, J. Phys. Earth, Vol.33, pp.59-96.

Horike, M., H. Uebayashi, and Y. Takeuchi [1990], ‘‘Seismic Response in Three-dimensional SedimentaryBasin Due to Plane S-wave Incidence’’, J. Phys. Earth. Vol. 38, pp. 261-284.

Horike, M. [1998], ‘‘Necessity, Planning, and Strategy of Underground Structure Determination at Megalopolis for Estimating the Site Effects from Future Earthquakes’’, Proc. of 2nd International Symposium on the Effects of Surface Geology on Seismic Motion, pp. 137-146.

Huang, N. E., and S. S. P. Shen [2005], *‘‘Hilbert-Huang Transform and Its Applications’’,* World Scientific Publishing Co. Pte. Ltd. , London, U.K.

Kinoshita, S. [1998], ‘‘Fuchu array –review’’, Proc. of 2nd international symposium on the effects of surface geology on seismic motion, pp.285-292.

Kinoshita, S. [2009], ‘‘Nonstationary ray decomposition in a homogeneous half space’’, Earth Planets Space, Vol.61, pp.1297-1312.

Langston, C. A. [1979], ‘‘Structure under Mount Rainier, Washington, inferred from teleseismic body waves’’, J. Geophys. Res., Vol. 84, pp.4749-4762.

Midorikawa, S. [2005], ‘‘Dense Strong – Motion Array in Yokohama, Japan, and Its Use for Disaster Management’’, Direction in Strong Motion Instrumentation, pp.197-208.

Miura, H., and S. Midorikawa [2001], ‘‘Effects of 3 D Deep Underground Structure on Characteristics of Rather Long Period Ground Motion Examination in and around Yokohama City’’, Zisin, 2, Vol. 54, pp.381-395 (in Japanese).

Nakahara, H. [2006], ‘‘Theoretical background of retrieving the Green’s function by cross correlation: One-dimensional case’’, Geophys. J. Int., Vol. 165, pp.719-728.

Suzuki, H., and K., Omura [1999], ‘‘Geological and Logging Data of the Deep Observation Wells in the Kanto Region, Japan’’, Technical Note of the NIED. No.191 (in Japanese with English abstract).

Takagishi, M., and S. Kinoshita [2011a],’’Estimation of Velocity Discontinuities in Sediment of Yokohama Region, Japan Using Yokohama Array Recordings for the 2011 off the Pacific Coast of Tohoku Earthquake (Mw=9.0)’’, Japan Geoscience Union Meeting 2011, Abstract MIS036-P073.

Takagishi, M., and S. Kinoshita [2011b], ‘‘Estimation of Velocity Boundaries in a Sedimentary Layer-Basement System Using the FCH Array Recordings – Evaluation of Nonstationary Ray Decomposition Method -’’, Zisin, 2, Vol. 64, No.1, in press (in Japanese).

Takahama, H., S. Abe, T. Nakajima, and S. Inui [2002], ‘‘Investigation of Deep Subsurface Structure Using the High Dense Strong Motion Seismograph Network’’, Journal of JAEE, Vol. 2, No.2, pp.23-40 (in Japanese with English abstract).

Toriumi, I. [1980], ‘‘Seismic Characteristics in the Osaka Plain’’, Summaries of technical papers of annual meeting, Architectural institute of Japan, pp.487-488.

Yamamizu, F. [2004], ‘‘Seismic Wave Velocity Structures in Kanto Area as Revealed by the Crustal Activity Observation Well VSP’’, Technical note of the NIED, No.251 (in Japanese with English abstract).

Yamamizu, F., H. Takahashi, N. Goto, and Y. Ohta [1981], ‘‘Shear Wave Velocities in Deep Soil Deposits Part 3 Measurements in the Borehole of the Fuchu Observatory to the Depth of 2, 750 m and a Summary of the Results’’, Zisin, 2, Vol.34, pp.465-480 (in Japanese).

Yoshimoto, K., N. Hirata, K. Kasahara, S. Sakai, K. Obara, T. Tanada, H. Nakahara, S. Kinoshita, and H. Sato [2010], ‘‘Seismic basement structure beneath the Metropolitan Tokyo area inferred from pseudo seismic reflection profiles’’, Japan Geoscience Union Meeting 2010, Abstract SSS024-10.

Zheng, H., K. Megawati, and S. Kinoshita [2011], ‘‘Application of Nonstationary Ray Decomposition to Identify Deep Seismic Bedrock of the Kanto Sedimentary Basin, Japan’’, Bull. Seism. Soc. Am., in press.